

Effects of functionalization conditions of sulfonic acid grafted SBA-15 on catalytic activity in the esterification of glycerol to monoglyceride: a factorial design approach

Lilis Hermida · Ahmad Zuhairi Abdullah ·
Abdul Rahman Mohamed

Published online: 30 November 2011
© Springer Science+Business Media, LLC 2011

Abstract A series of propyl sulfonic acid-modified SBA-15 catalysts (SBA-15SO₃H) was prepared under various conditions using post-functionalization approach. A factorial design coupled with response surface analysis were employed to evaluate the effects of the preparation conditions on the catalyst activity. Optimization of the conditions to find the most active SBA-15SO₃H catalyst with the highest activity in glycerol esterification with lauric acid at 160 °C for 6 h was also made. Amount of 3-(mercaptopropyl)trimethoxysilane (MPTMS) and reflux time were chosen as parameters of the preparation conditions. The presence of propyl sulfonic acid groups in SBA-15SO₃H catalysts was confirmed by FT-TIR method. The catalysts were also characterized by means of surface analysis, XRD, TEM and TGA. The results obtained from the statistical models suggested that the amount of MPTMS was more important parameter to influence the activity compared to the reflux time. The optimum preparation condition was achieved at a reflux time of 20 h and an MPTMS amount of 1 mL/gram SBA-15 to obtain the SBA-15SO₃H(1) with the highest monoglyceride selectivity (70.2%) and corresponding lauric acid conversion (95%) in the esterification process.

Keywords Sulfonic-SBA-15 · Post-synthesis functionalization · Factorial design · Glycerol esterification · Monoglyceride · Process intensification

L. Hermida · A. Z. Abdullah (✉) · A. R. Mohamed
School of Chemical Engineering, Universiti Sains Malaysia,
Engineering Campus, 14300 Nibong Tebal, Penang, Malaysia
e-mail: chzuhairi@eng.usm.my

L. Hermida
Department of Chemical Engineering, Universitas Lampung,
Bandar Lampung 35145, Lampung, Indonesia

1 Introduction

Rapid increase in biodiesel production produces an excess of glycerol as a co-product. Oversupply of glycerol reduces its price. The low cost and an increase in glycerol availability definitely justify the efforts to convert it into value-added products. Monoglyceride that can be prepared via esterification or transesterification of glycerol has significant applications as safe and biodegradable emulsifiers in industrial products [1]. Its applications can be found in food industries, cosmetic products, pharmaceutical formulations, drug delivery systems, oil well drilling systems, textiles, packaging materials, plastic processing and construction materials. Monoglyceride or its mixture with di-glyceride accounts for about 75% of the worldwide emulsifier production [2]. The global production of emulsifier is estimated to be at approximately 200,000–250,000 metric tons per year [3]. Recently, transformation of glycerol into monoglyceride through transesterification of glycerol with fatty acid methyl ester has been reported [4]. The transesterification process was favorable at high reaction temperatures (220–250 °C) using MgO as the catalyst. Besides that, monoglyceride can also be produced via esterification of glycerol with fatty acid at a lower reaction temperature (<180 °C) [5].

Commercial esterification processes usually rely on strong homogeneous mineral acid catalysts such as sulfuric acid, hydrochloric acid or orthophosphoric acid [6, 7]. However, this energy intensive technology creates large amounts of by-products or waste [8]. In many aspects, solid acid catalysts offer several advantages over those homogeneous acid catalysts due to the avoidable corrosion problem and non-reusability of the latter group of catalysts [9].

Acidic resins and zeolites with small pore diameters of less than 8 Å had been used as solid acid catalysts for monoglyceride production [10–12]. However, acidic resins were unfavorable as they were found to be highly susceptible to swelling in organic solvents and unstable at elevated reaction temperatures (>150 °C). Meanwhile, catalytic activity of the zeolites was low to favor monoglyceride formation. The problem was due to their small pore diameters which caused severe restriction for the formation and diffusion of bulky monoglyceride molecules [13].

Recently, mesoporous silicas (pore sizes between 20 and 100 Å) received a lot of attention as fascinating functional materials can be created through the incorporation of various substances such as organic molecules or metal nanoparticles into their pores [14]. MCM-41 mesoporous material that had been incorporated with propyl sulfonic acid was reported to be an excellent acid catalyst for formation of bisfurylalkanes and polyol esters [15]. However, this mesoporous material has a severe drawback of low thermal stability.

SBA-15 mesoporous materials generally show high thermal stability. This material had been incorporated with Au/TiO₂ to generate solid catalyst. This catalyst exhibited high activity in the hydrodechlorination of carbon tetrachloride (CCl₄) [16]. SBA-15 mesoporous materials had also been incorporated with propyl sulfonic acid to create acid sites via direct synthesis method (in situ functionalization) for the esterification of glycerol with oleic acid [17]. It was however reported that the SBA-15SO₃H catalyst gave a rather poor catalytic activity due to the presence of some acid sites in the micropores of the SBA-15SO₃H catalyst. This caused a lower availability of acid centers to reactant molecules.

Post-synthesis modification (grafting) that involves synthesizing SBA-15 silica materials followed by subsequent surface functionalization allows the synthesis of modified SBA-15 with highly ordered silica geometries even at moderately high acid loadings to create good solid acid catalysts [18, 19]. This promises better catalytic activity as microporosity will be kept to the minimum. In the present study, a series of propyl sulfonic acid functionalized SBA-15 catalysts (SBA-15SO₃H) were prepared through a post-synthesis modification method and their catalytic activities were subsequently tested for glycerol esterification with lauric acid. The reaction was performed in solvent-free condition at 160 °C for 6 h with molar ratio of glycerol/lauric acid of 4:1. Behaviors in the esterification process were comparatively studied using the synthesized catalysts.

In this modification, the amount of 3-(mercaptopropyl)trimethoxysilane (MPTMS) and reflux time were deemed as the most influential factors to affect the

characteristic of SBA-15SO₃H catalysts and consequently their catalytic activity. Effects of both factors on the catalytic activity were evaluated using a 3² factorial design coupled with response surface analysis. Optimization of the preparation conditions was also carried out to obtain the most active SBA-15SO₃H catalyst.

2 Materials and methods

2.1 Preparation of SBA-15SO₃H catalysts

Pure siliceous SBA-15 materials used in this study were synthesized according to a method described in literature [20] with modifications. In a typical preparation method, 4 g of Pluronic P123 tri-block co-polymer (Aldrich, 99%) i.e. poly(ethylene glycol)-(propylene glycol)-poly(ethylene glycol) was first dissolved in water (30 mL) and 2 M HCl (120 mL) at room temperature. The solution temperature was then raised to 60 °C. Next, 8.50 g of tetraethyl orthosilicate (TEOS) (Merck, 99.5%) was added to the solution under a rapid stirring for 30 min and a precipitated product appeared. The stirring rate was then decreased and the reaction system was kept under this condition for another 20 h. After that, the content was transferred to a polyethylene bottle and aged at 80 °C for 48 h in an oven under static condition. After cooling to room temperature, the solid product was filtered, washed with deionized water, dried in air at room temperature for 12 h and then dried in oven at 100 °C for another 12 h. Then, calcination was carried out in static air at 300 °C for 0.5 h and then at 550 °C for 6 h to obtain the parent SBA-15.

Next, 1 gram of SBA-15 that was previously heated at 120 °C for 4 h to properly dry it and desorb any adsorbed gases that could influence the subsequent functionalization process was added into 25 mL of dry toluene under mild stirring. Then, 3-MPTMS was added at various amounts (1, 3, and 5 mL per gram of SBA-15) and the resulting mixtures were refluxed between 4 and 20 h to obtain a propyl thiol groups-modified SBA-15. The solids were then filtered and washed with acetone. The materials were then subjected to soxhlet extraction with ethanol for 24 h and subsequently dried in air. Then, the thiol groups (–SH) were converted to SO₃H groups by oxidation with 20 mL of 30 wt% H₂O₂ solution under continuous stirring at 60 °C for 24 h. Then, the solid was filtered off, washed with water and ethanol and then acidified under reflux condition with 17.5 mL of 10% (w/w) H₂SO₄. After that, the mixture was filtered off, washed thoroughly with water, and then dried at 100 °C for 12 h. Hereafter, the synthesized catalysts will be denoted as SBA-15SO₃H(N), where N is the experimental number.

2.2 Factorial design

Statistical experimental designs [21] are very efficient method for observing systems that depend on several factors. A 3^2 factorial design that is one of the statistical designs has been successfully used to study the influence of different factors on activity of a novel solid catalyst [22]. In the present study, the 3^2 factorial design was chosen as the statistical experimental design in which preparation factors affecting the catalyst activity were the amount of MPTMS and reflux time. To perform the experimental design work, a Design-Expert software package (version 6.0.6, Stat Ease, Inc., USA) was used. The synthesis conditions were selected based on findings made in previous studies of post synthetically produced sulfonic acid functionalized MCM-41, SBA-15 and FSM-16 [23–26]. The design in coded (a and b) and actual (A and B) independent variables are summarized in Table 1. Low and high levels of each variable are denoted as -1 and $+1$, respectively while the central values of the variable are coded as 0. The three levels of each parameter are also given in Table 1.

2.3 Characterization of catalysts

Pore size distribution was obtained from the nitrogen adsorption–desorption isotherms of the parent SBA-15 and SBA-15SO₃H samples. The N₂ adsorption–desorption measurements were performed using a Quantachrome Autosorb-1 equipment. Prior to the adsorption–desorption process, the samples were degassed ($P < 10^{-1}$ Pa) at 270 °C for 6 h. Surface area was calculated using the BET method (S_{BET}) while the pore size distribution was determined using the Barrett-Joyner-Halenda (BJH) model applied to the adsorption branch of the isotherm. The micropore area (S_{μ}) was estimated using the correlation of *t*-Harkins and Jura (*t*-plot method).

Table 1 The 3^2 factorial experimental matrix

Experimental number	Sample	Coded		Actual	
		a	b	A	B
1	SBA-15 SO ₃ H(1)	+1	−1	20	1
2	SBA-15 SO ₃ H(2)	+1	0	20	3
3	SBA-15 SO ₃ H(3)	+1	+1	20	5
4	SBA-15 SO ₃ H(4)	−1	−1	4	1
5	SBA-15 SO ₃ H(5)	−1	0	4	3
6	SBA-15 SO ₃ H(6)	−1	+1	4	5
7	SBA-15 SO ₃ H(7)	0	−1	12	1
8	SBA-15 SO ₃ H(8)	0	0	12	3
9	SBA-15 SO ₃ H(9)	0	+1	12	5

A: Reflux time, h

B: MPTMS amount, mL per gram of SBA-15

Fourier-transform infrared (FTIR) spectrums were recorded on a Perkin-Elmer 2000 system using the KBr wafer technique. Small-angle X-ray diffraction (XRD) analysis was performed on a Siemens 2000X system using the CuK α . Morphology of samples was observed by means of field emission scanning electron microscope (FESEM) using a JEOL-SM7600F equipment. The FESEM images were taken directly from samples without altering or coating the samples at a magnification of 200,000 \times and a low accelerating voltage of 0.5 kV. Transmission electron microscopy (TEM) studies were performed using a Philips CM 12 transmission electron microscope. Meanwhile, thermal gravimetric analysis (TGA) was also performed to determine the amount of weight loss of samples as they were heated. TGA investigation was carried out using a thermal gravimetric analyzer unit coupled with a TG controller (TAC 7/DX) that was supplied by Perkin-Elmer, USA. About 5 mg of catalyst sample was heated from 31 to 840 °C with heating rate of 10 °C/min and an air flow rate of 25 mL/min.

2.4 Activity studies

The catalytic activity of SBA-15SO₃H catalysts for glycerol esterification with lauric acids was carried out in a two-necked flask reactor equipped with a stirrer, a thermometer and a tube connected with a vacuum pump. A desired working pressure was maintained by means of a vacuum pump. This system readily permitted the elimination of water without significant variation in reaction volume [5]. The whole reactor was immersed in a constant temperature bath.

The reactants i.e. lauric acid (0.026 mol) and glycerol (0.105 mol) and the catalyst (0.75 g) were first added to the reactor. Before an experiment was started, the system was bubbled with nitrogen to create an inert environment for the reaction. The reaction mixture was then heated to 160 °C after the desired reduced pressure was reached (50.8 cm Hg). Then rapid stirring was started and the reactants were stirred for 6 h.

2.5 Product analysis

The product mixtures were analyzed by means of a gas chromatograph (Agilent 7820A system) equipped with a (15 m \times 0.32 mm \times 0.10 μ m) CP Sil 5CB capillary column. Sample analysis method was adapted from a literature report [27]. The detector and injector were set to operate at 380 and 250 °C, respectively while the column temperature was initially maintained at 80 °C for 1 min and was then programmed at 15 °C/min to 330 °C, and maintained at the final temperature for another 2 min. 100 μ L of samples were withdrawn from the reactor at the desired interval and

added to a vial containing 100 μL of water and 100 μL of methyl acetate. The contents were then vortexed and the organic phase was separated by means of centrifugation. Next, 20 μL of the organic phase was dissolved in 480 μL of acetone and 100 μL of 0.2 M pentadecanoic acid as the internal standard. Direct injection of the samples was carried out into the gas chromatograph. Detail description on the analysis method is available in our previous work [26].

Esterification of glycerol with fatty acid to produce monoglyceride is a reversible reaction and the stoichiometry of the esterification requires glycerol/fatty acid molar ratio of 1:1. In the present study, the glycerol esterification was carried out under excess glycerol i.e. glycerol/fatty acid molar ratio of 4:1, with the continuous removal of water from the reaction system. On the basis of this reaction condition, reaction steps for the glycerol esterification with fatty acid were irreversible parallel reactions to produce monoglyceride and by-products of diglyceride and triglyceride (see Fig. 1) as reported in the literature [5]. Hence, the conversion of lauric acid was expressed on the basis of lauric acid transformation using the reaction coefficients for the formation of mono-, di- and triglycerides [12] as given in Eq. 1. In the same approach, the selectivity of monoglyceride was expressed by the ratio of the ester to all the various reaction products (corrected by the reaction coefficients) as given in Eq. 2.

$$\text{Conversion (\%)} = \frac{[(C_M + 2C_D + 3C_T)/(C_M + 2C_D + 3C_T + C_A)] \times 100}{(1)} \quad (1)$$

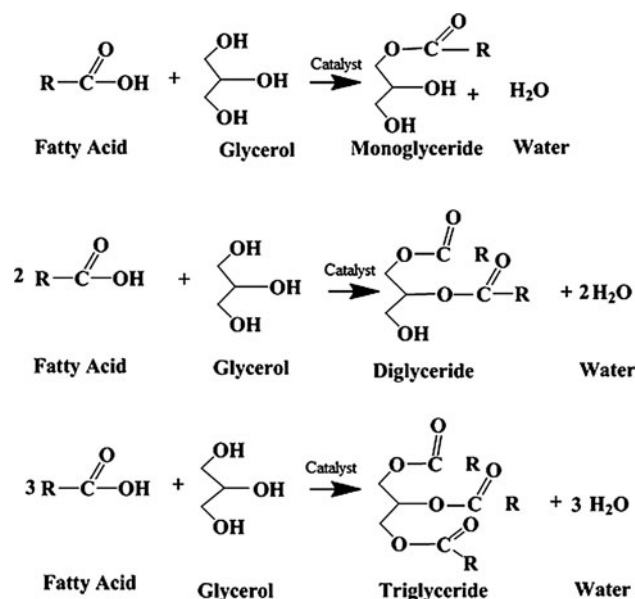


Fig. 1 Irreversible parallel reactions of glycerol esterification with fatty acid to produce monoglyceride and the formation of diglyceride and triglyceride as by-products

$$\text{Monoglyceride selectivity (\%)} = \frac{[C_M / (C_M + 2C_D + 3C_T)] \times 100}{(2)}$$

where, C_A = Concentration of lauric acid, mol/L; C_M = Concentration of monoglyceride, mol/L; C_D = Concentration of diglyceride, mol/L; C_T = Concentration of triglyceride, mol/L.

3 Results and discussion

3.1 Characterization of the catalysts

In post-synthesis grafting approach as used in this work, modification of mesoporous silica was carried out by silylation of the organosilane with surface silanol on mesoporous surface as schematically shown in Fig. 2. It should be noted that the silanol groups could occur on the microporous and mesoporous pores of the material so that the acid functional group could present on both categories of pores. By maintaining the straight hexagonal channels of SBA-15, more acid sites were deemed to have been introduced on the mesopores rather than micropores.

FT-IR spectrum of the parent SBA-15 material as shown in Fig. 3 shows vibrations at around 1,060–1,260, 820 and 500 cm^{-1} to indicate Si–O–Si stretching vibrations. The evidence for the presence of propyl sulfonic acid group in SBA-15SO₃H was confirmed by the presence of additional vibrations at 650 cm^{-1} that was attributed to the C–SO₃H stretching vibrations. Besides, additional vibrations were also detected at around 2,928, 2,852 and 1,465 cm^{-1} . The wave numbers at 2,928 and 2,852 were attributed to CH₂ stretching vibrations while that occurred at 1,465 cm^{-1} corresponded to CH₂ bending vibrations [28].

It can be seen that C–SO₃H stretching vibrations at 650 cm^{-1} and CH₂ stretching vibrations at 2,928, 2,852 and 1,465 cm^{-1} of the catalysts prepared using MPTMS amount of 1 mL per gram SBA-15 (i.e. SBA-15SO₃H(1) and SBA-15SO₃H(7)) were stronger than those of the catalysts prepared using MPTMS amount of 3 mL (i.e. SBA-15SO₃H(2) and SBA-15SO₃H(8)) and 5 mL (i.e.

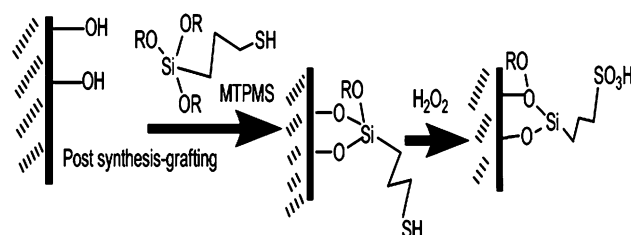


Fig. 2 Post synthesis grafting method for the preparation of SBA-15 functionalized with propylsulfonic acid

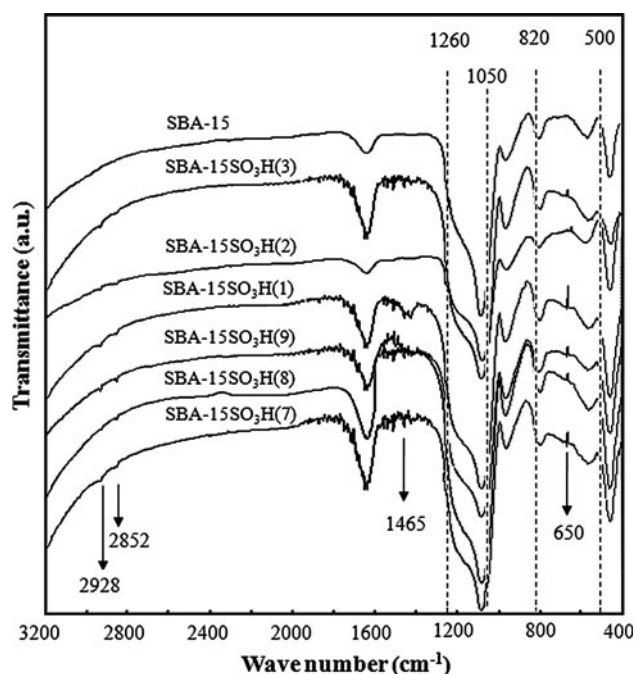


Fig. 3 FTIR spectra of parent SBA-15 and SBA-15 functionalized with propylsulfonic acid

SBA-15SO₃H(3) and SBA-15SO₃H(9)). This trend suggested that the catalysts prepared using the 1 mL MPTMS amount had the most propyl sulfonic acid groups which were successfully grafted on the surface [6, 9, 15]. Meanwhile the stretching vibrations of the catalysts prepared using the 5 mL of MPTMS were stronger than those of the catalysts prepared using the 3 mL MPTMS amount. It therefore could be concluded that the amount of propyl sulfonic acid successfully grafted on the SBA-15 material increased in the order of: 3 mL MPTMS/g < 5 mL MPTMS/g < 1 mL MPTMS/g. This result suggested that there was some kind of interaction between the amount of MPTMS and reflux time on the degree of acid functionalization into SBA-15.

The structure of SBA-15 consists of hexagonal packing of cylindrical mesopores which are interrelated randomly by micropores that present in the pore walls [29]. The surface characteristics of the parent SBA-15 and SBA-15SO₃H catalysts prepared through different conditions are presented in Table 2. The table shows that the amount of micropores in the SBA-15SO₃H catalysts was lower compared to that in the parent SBA-15. This result suggested that acid functionalization could be responsible for the elimination of microporosity in the pore walls. Meanwhile, the average pore diameters of the modified samples had a tendency to be higher than the corresponding values for the parent SBA-15. The increasing trend in the pore diameter after acid functionalization indicated that the preparation conditions used allowed the enlargement of mesoporous structure of the SBA-15 [30]. This was attributed to the grafting of sulfonic acid groups on the mesoporous walls. It should also be noted that despite of having a higher average pore diameter, the SBA-15SO₃H(1) had a higher total surface area compared to that of the parent SBA-15. This finding suggested that the preparation conditions using MPTMS amount of 1 mL per gram SBA-15 and at reflux time of 20 h allowed restructuring in the hexagonal structures of the SBA-15SO₃H(1) catalyst. This restructuring resulted in significant disappearance of micropore structures.

Despite having smaller average pore diameter compared to the parent SBA-15, SBA-15SO₃H(4) also had higher surface area. A plausible explanation for the smaller pore diameter of SBA-15SO₃H(4) was that upon grafting of the lowest MPTMS amount (1 mL per gram SBA-15) and at the shortest reflux time (4 h), the silylation mainly took place inside the pore structures of the catalyst. Moreover, the restructuring and enlargement of the hexagonal structure of the SBA-15SO₃H(4) by maintaining the ordered hexagonal pore structure resulted in the high increase in mesopore area and a slight decrease in micropore structures. The reductions of average pore size and micropore

Table 2 Surface characteristics of the parent and modified silica materials

Silica materials	Total surface area ^a , m ² /g	Micropore area ^b , m ² /g	Mesopore area ^a , m ² /g	Average pore diameter ^a , Å	Total pore volume ^a , cc/g
SBA-15	542	149	393	58.7	0.795
SBA-15SO ₃ H(1)	607	79	528	67.2	1.018
SBA-15SO ₃ H(2)	449	72	337	65.5	0.736
SBA-15SO ₃ H(3)	494	60	433	65.9	0.814
SBA-15SO ₃ H(4)	632	109	522	32.7	1.035
SBA-15SO ₃ H(5)	499	70	428	65.6	0.818
SBA-15SO ₃ H(6)	485	103	382	71.5	0.868
SBA-15SO ₃ H(7)	431	78	352	64.4	0.695
SBA-15SO ₃ H(8)	531	89	441	65.8	0.874
SBA-15SO ₃ H(9)	503	87	415	66.4	0.836

^a Using the BET equation (S_{BET})

^b Using the t-Harkins and Jura correlation (t-plot method)

structure in SBA-15SO₃H(4) could also be confirmed by pore size distributions as shown in Fig. 4.

The pore size distributions of the SBA-15 and SBA-15SO₃H catalysts in Fig. 4 were analyzed with the desorption branch using BJH method. The figure shows strong evidences that pore size diameter at the maximum peak in SBA-15SO₃H(4) was smaller than that in parent SBA-15. Meanwhile, the distribution of micropore structure in the SBA-15SO₃H(4) was lower compared to that in SBA-15. In addition, Fig. 4 confirms that the SBA-15 SO₃H(1) catalyst had more defined structure with higher pore size diameter at the maximum peak than that of the parent SBA-15. This finding was in agreement with surface characteristic results as shown in Table 2.

Successful grafting of sulfonic functional group is usually reported to cause a slight increase in average pore size of mesoporous materials due to the inclusion on sulfonic acid in the mesopores so that the mesoporous channels swell a bit. In this work, SBA-15SO₃H(4) was synthesized at low levels of the variables tested i.e. 4 h of reflux at a MPTMS loading of 1 mL/g SBA-15. This result was an indication of low degree of functionalization.

Nitrogen adsorption–desorption isotherm curves for the parent SBA-15 and modified SBA-15 are depicted in Fig. 5. All curves in the figure exhibited type IV isotherms, implying that they were materials with sufficiently ordered mesostructures. The results suggested that the mesoporous nature of the material was preserved even after the grafting

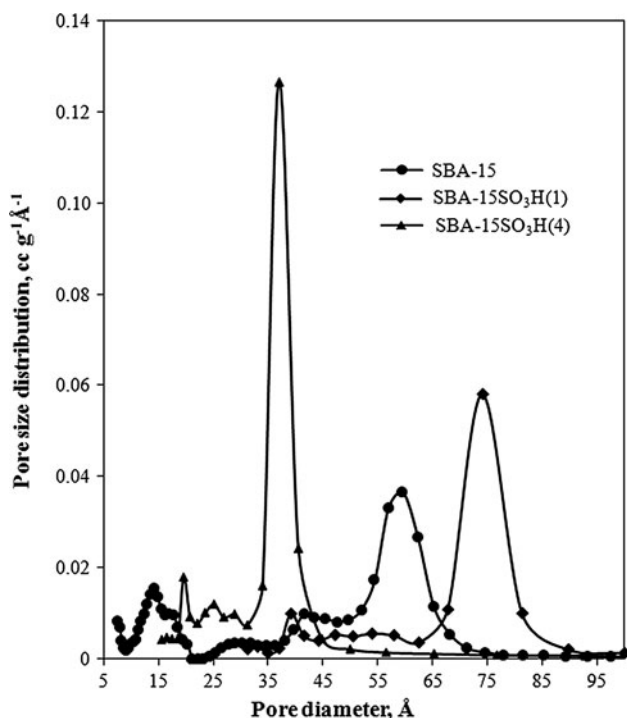


Fig. 4 BJH pore size distributions for the parent SBA-15 and sulfonic acid-modified SBA-15

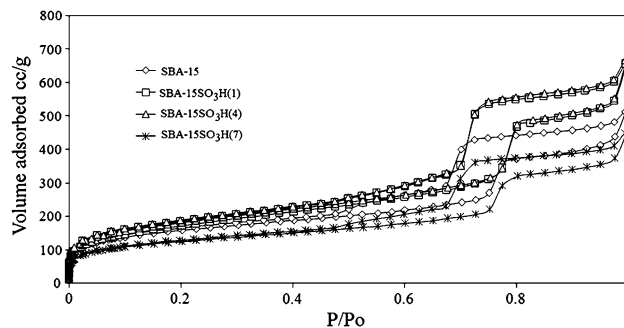


Fig. 5 N₂ adsorption–desorption isotherms for the parent SBA-15 and sulfonic-acid modified SBA-15

of propyl sulfonic acid groups. Thus, it could be concluded that the grafting mainly occurred on the external surface (grafted on silanol groups) without much disturbance on the silica network.

The mesoporous structure that was maintained after post synthesis-grafting of the organo sulfonic groups was also proven by XRD analysis as shown in Fig. 6. In this study, XRD patterns of the parent SBA-15 and the modified SBA-15 were recorded at 2θ angles from 1.1° to 10°. The patterns of all samples featured intense peaks at 1.5°–2° identified as (110) and (200) reflections associated with *p6mm* hexagonal symmetry. Meanwhile, the (100) diffraction peaks were not detected. It was because the XRD diffractometer used in this study was not capable of determining peaks at 2θ angles of about 1° or lower where the (100) diffraction peaks were generally observed [29, 31]. Thus, the (200) interplanar spacing, d_{200} , was used

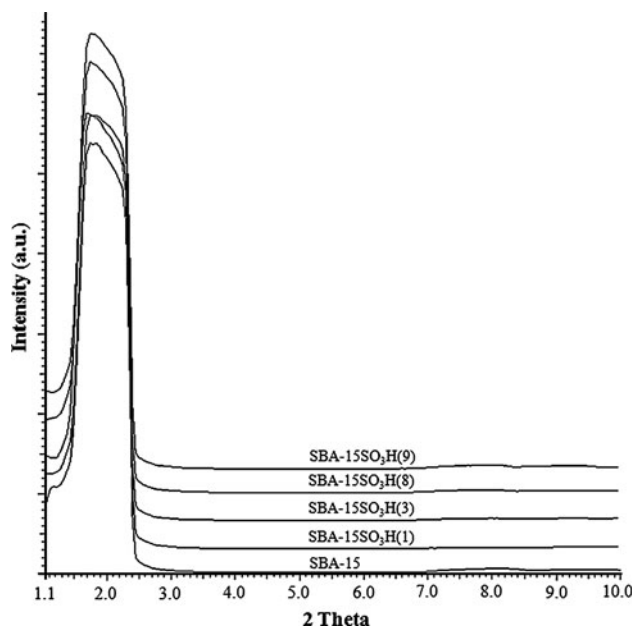


Fig. 6 XRD patterns of parent SBA-15 and the sulfonic acid-modified SBA-15

instead of the (100) interplanar spacing, d_{100} , for the estimation of unit-cell parameter, a . This parameter corresponds to the distance between the centres of adjacent mesopores according to the formula, $a = 4 \times 3^{-1/2} d_{200}$ [29]. The unit-cell parameters of SBA-15 and SBA-15 functionalized with organosulfonic acid catalysts are shown in Table 3. The unit-cell parameter results in the table indicate that there was no significant difference in the XRD patterns for the parent SBA-15 and the modified SBA-15 catalysts.

TEM images of the parent SBA-15 and SBA-15SO₃H(1) are presented in Fig. 7. The images were to the confirmation of well-ordered hexagonal arrays of one dimensional mesopores structure in the parent SBA-15 is presented in Fig. 7a. SBA-15SO₃H(1) showed that the structure remained nearly the same after acid functionalization (Fig. 7b). Based on FTIR result, it was clear that propyl sulfonic acid groups were successfully incorporated in the SBA-15 after the post-synthesis functionalization procedure. Thus, it was confirmed that the functionalization occurred without significant changes to the mesoporous structure of SBA-15. The SBA-15SO₃H(1) catalyst retained the uniformity of the mesopore channels as shown by the parent SBA-15.

Figure 8 shows TGA results of parent SBA-15 and SBA-15SO₃H(1). Thermal gravimetric profile of SBA-15 material shows about 20% weight loss of the sample weight below 100 °C, which corresponded to the desorption of physically adsorbed water. Meanwhile, the thermal gravimetric profile of SBA-15SO₃H(1) catalyst had notable two steps of weight loss. The first weight loss, i.e. about 20% of the sample weight was ascribed to water removal. The second weight loss of about 7.5% of the sample weight at temperatures from 300 to 650 °C mainly indicated the decomposition of the propyl sulfonic acid in SBA-15SO₃H(1) catalyst. The temperature range of this

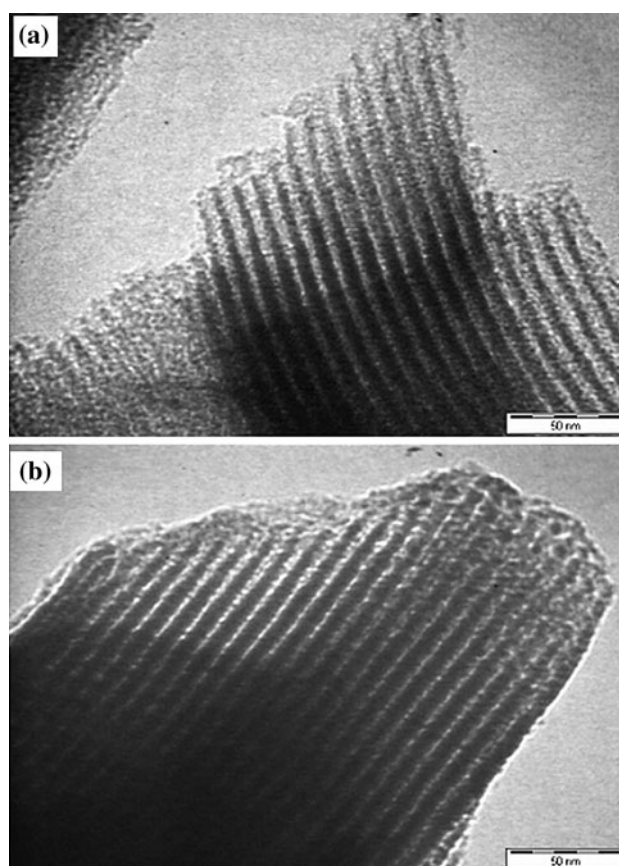


Fig. 7 TEM images of **a** parent SBA-15, **b** SBA-15 SO₃H(1) at a magnification of 5 kX

decomposition was similar to that previously reported [27]. In addition, there was no significant change in the weight of the catalyst at 160 °C. This observation suggested that the SBA-15SO₃H(1) catalyst should be stable for the glycerol esterification with lauric acid at 160 °C as used in the present study.

In this study, direct quantification of the degree of sulfonic acid functionalization based on TGA results would subject to significant error as sharp weight difference could not be measured. A very gradual weight low was generally observed and the temperature at which the decomposition ended could not be clearly seen. This measurement was further complicated due to small difference in the degree of functionalization between the samples. Thus, for the sake of clarify, only results with SBA-15 and SBA-15SO₃H(1) are shown in Fig. 8.

3.2 Model fitting and statistical analysis

The responses for evaluation of the SBA-15SO₃H catalysts prepared was their activity in the glycerol esterification with lauric acid at 160 °C for 6 h were measured in terms of the lauric acid conversion and monoglyceride

Table 3 Surface characteristics of the parent SBA-15 and SBA-15SO₃H catalysts

Silica material	d_{200} , Å	Unit-cell parameter (a), Å
SBA-15	62.06	143.3
SBA-15SO ₃ H(1)	63.01	145.5
SBA-15SO ₃ H(2)	63.01	145.5
SBA-15SO ₃ H(3)	63.01	145.5
SBA-15SO ₃ H(4)	63.01	145.5
SBA-15SO ₃ H(5)	63.01	145.5
SBA-15SO ₃ H(6)	63.01	145.5
SBA-15SO ₃ H(7)	62.06	143.3
SBA-15SO ₃ H(8)	63.01	145.5
SBA-15SO ₃ H(9)	62.06	143.3

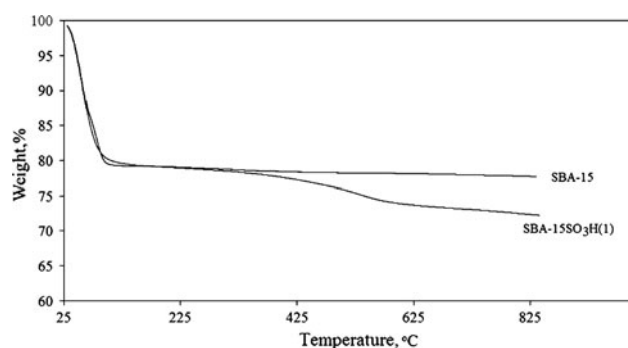


Fig. 8 Thermal gravimetric analysis results of parent SBA-15 and SBA-15SO₃H(1)

selectivity. The values of the experimental results are given in Table 4. By assuming a second order polynomial model, predictive Eqs. 3 and 4 for the responses were produced by the software used, where A and B represent the reflux time and MPTMS amount, respectively, C corresponds to lauric acid conversion and S corresponds to monoglyceride selectivity. The influence of the parameters and their combination are related to the value and sign of the polynomial expressions, as follows:

$$C = 68.44 + 4.58A - 6.13B - 0.15A^2 + 0.96B^2 + 0.026A * B; \\ R^2 = 0.97 \quad (3)$$

$$S = 54.05 - 2.91A + 18.29B + 0.23A^2 - 4.66B^2 \\ + 0.066A * B - 0.096A^2 * B - 0.36A * b^2; \\ R^2 = 0.99. \quad (4)$$

Equations 3 and 4 satisfactorily fitted the experiment data obtained. The values of the responses calculated from the models are also given in Table 4. In addition, Figs. 9 and 10 show the relationship between the experimental and predicted response values. The values calculated by the predictive equations as presented in Figs. 9 and 10 are very close to the experimental values obtained with an R^2 value

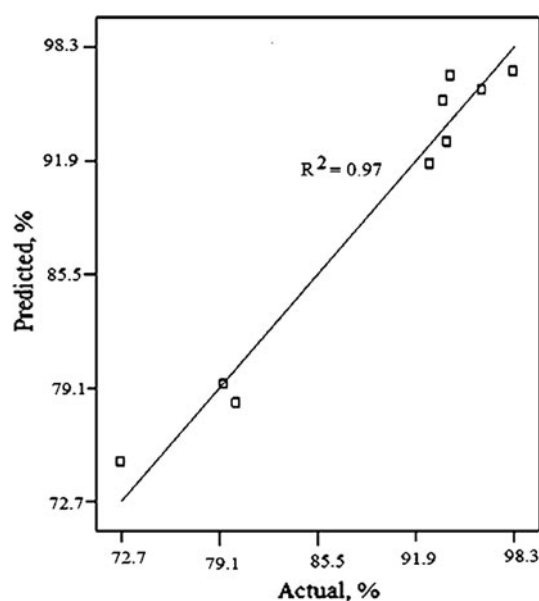


Fig. 9 Accuracy of the predicted lauric acid conversions versus experimental values

of 0.97 and 0.99, respectively. The R^2 value determines the relevance of the dependent variables in the models in explaining the behaviour of variations. The closer the value of R^2 to unity, the better empirical models are in fitting the experiment data [32]. The results suggested the accuracy and reliability of these equations in representing the esterification reaction over a wide the range of catalyst preparation conditions.

Table 5 and Table 6 show statistical data acquired from analyses of variance (ANOVA) for the quadratic models of Eqs. 3 and 4. Value of “ $P > F$ ” of less than 0.05 indicates that the model has significant effects on the response. On the other hand, a value of “ $P > F$ ” of greater than 0.100 indicates that the model term has no significant effects [21]. Table 5 and Table 6 show that the values of $P > F$ are 0.02 and 0.0083, respectively. This indicates that there is only 2% chance that a “model F -value” this large

Table 4 Factorial design experimental conditions and corresponding results

Reflux time, h	MPTMS amount, mL	Lauric acid conversion, %		Selectivity to monoglyceride, %	
		Experimental	Calculated	Experimental	Calculated
20	1	93.71	95.25	70.23	70.29
20	3	92.85	91.70	53.19	53.22
20	5	96.23	95.84	56.75	56.74
4	1	79.42	79.29	59.85	59.84
4	3	72.72	74.91	68.13	68.16
4	5	80.27	92.93	50.79	50.78
12	1	98.30	96.89	56.67	56.70
12	3	93.98	92.93	64.68	64.62
12	5	94.20	96.65	69.97	69.99

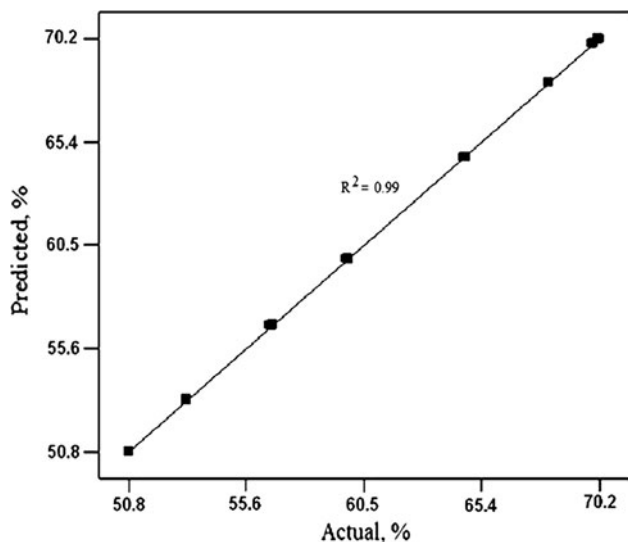


Fig. 10 Accuracy of the predicted monoglyceride selectivities versus experimental values

could occur due to noise for the lauric acid conversion response and there was only 0.83% chance for monoglyceride response. Therefore A, B, A², B² and AB were significant model terms in affecting the lauric acid conversion. Meanwhile, monoglyceride selectivity was greatly influenced by the significant model terms i.e. A, B, A², B², AB, A²B, and AB².

3.3 Effect of the preparation parameters on catalyst performance

3.3.1 Lauric acid conversion

Equation 3 shows the strongest influence of the linear factor of MPTMS amount (B) that gave significant negative effects on lauric acid conversion while their quadratic factor (B²) indicating excess of MPTMS proportion gave positive effects. On the other hand, the strong influence of the linear factor of reflux time (A) showed significant positive effects. The lauric acid conversion was also positively influenced by a two factor interaction i.e. A*B. The presence of this interaction indicates that the effect of A depended on the value of B.

3D response surface for lauric acid conversion against the reflux time (A) and the MPTMS amount (B) in conjunction with its contour plot is presented in Fig. 11. The 3D response surfaces shows that, at the lowest MPTMS, lauric acid conversion showed a significant increase with the first 16 h of reflux time and then reduced slightly when the reflux time was extended to 20 h. This can be explained from the surface characterization results in Table 2 that show an increase in lauric acid conversion as a consequence of a decrease in micropore area of the resulting the modified catalyst at about the first 16 h of reflux time. Then, the micropore area of the catalyst increased slightly until a reflux time of 20 h.

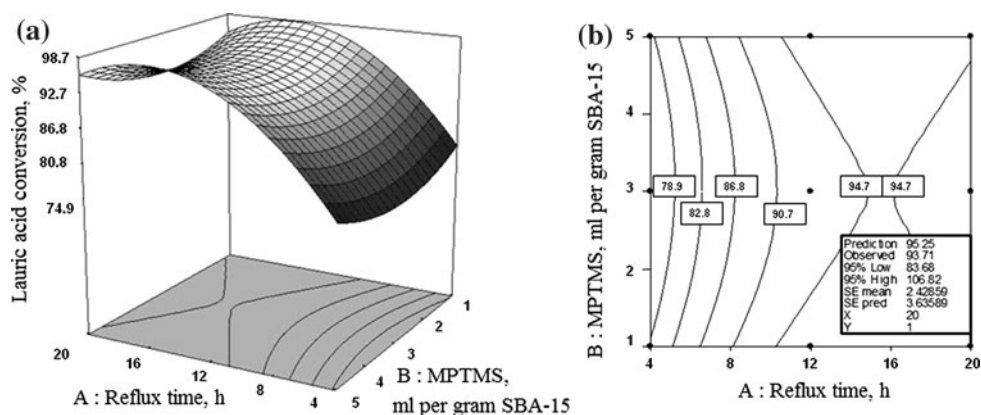
Table 5 ANOVA for quadratic model of Eq. 3

Source	SS	DF	MS	F _{Value}	Prob > F	
Model	638.6211	5	127.7242272	17.44462461	0.0200	Significant
Residual	21.96509	3	7.32169537			
Corr. total	660.5862	8				
Std. Dev.	2.705863		R-squared	0.9667491		
Mean	89.07556		Adj. R-squared	0.911330935		
C.V.	3.037717		Pred. R-squared	0.612323382		
Press	256.0938		Adeq. precision	9.950235209		

Table 6 ANOVA for quadratic model of Eq. 4

Source	SS	DF	MS	F _{Value}	Prob > F	
Model	433.2259	7	61.88941429	12630.49271	0.0069	Significant
Residual	0.0049	1	0.0049			
Corr. total	433.2308	8				
Std. Dev.	0.07		R-squared	0.99998869		
Mean	61.14		Adj. R-squared	0.999909517		
C.V.	0.114491		Pred. R-squared	0.997938685		
Press	0.893025		Adeq. precision	294.560482		

Fig. 11 Response surface plot for lauric acid conversion (a) and its contour plot (b)



Bulky monoglyceride molecules were unable to form and diffuse through microporous channel [11]. The increase in micropore area resulted in a decrease in lauric acid conversion because the acid sites were located inside the micropore structures became inaccessible. Similar explanation was applicable for the use of MPTMS of 3 and 5 mL per gram SBA-15, where lauric acid conversion was found to increase significantly with the reflux time of about 16 h. However, it decreased, at longer duration of reflux to suggest partial elimination of ordered mesoporous structure of SBA-15.

It was noted that within the range of reflux time studied, lauric acid conversion slightly reduced with the MPTMS amount of more than 1 mL per gram SBA-15. This finding was attributed to the more stacking faults in the SBA-15SO₃H catalysts prepared with the MPTMS amount more than 1 mL per gram SBA-15. This resulted in the lower amount of propyl sulfonic acid groups successfully grafted on the surface of the SBA-15 as proven by the FT-IR spectra analysis in Fig. 3. The figure indicates that the modified SBA-15 catalysts with MPTMS amount of 1 mL per gram SBA-15, such as SBA-15SO₃H(1) and SBA-

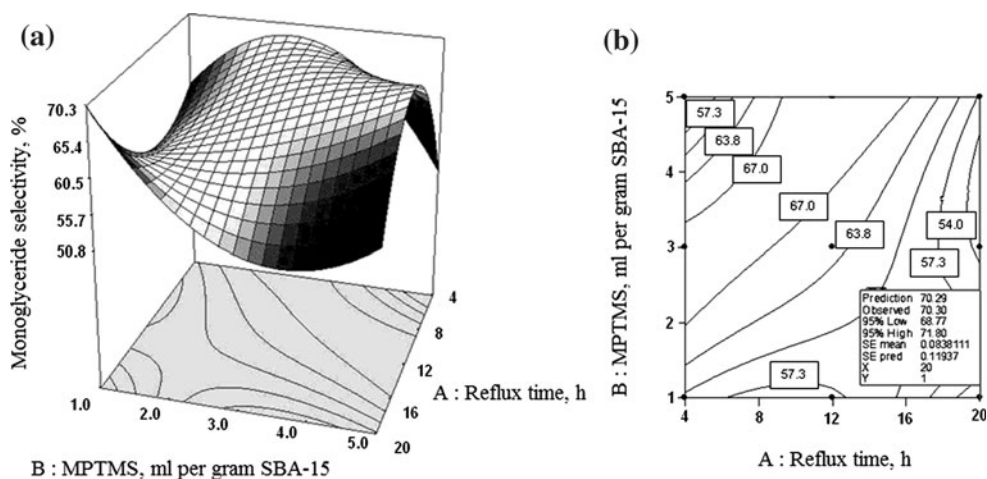
15SO₃H(7) showed stronger stretching vibrations compared to those of modified SBA-15 catalysts with higher amount of MPTMS (3 and 5 mL per gram SBA-15) i.e. SBA-15SO₃H(2), SBA-15SO₃H(8), SBA-15SO₃H(3), SBA-15SO₃H(9).

3.3.2 Selectivity to monoglyceride

As noted in Eq. 4, the strongest influence on monoglyceride selectivity was also a linear factor of MPTMS amount (B). This factor gave significant positive effects on monoglyceride selectivity although its quadratic factor (B^2) suggested that excess MPTMS amount had strong negative effects. The negative influence was also seen from the linear factor of reflux time (A) while its quadratic factor (A^2) gave positive effects. Two factor interactions i.e. $A*B$, A^2*B and $A*B^2$ indicated that the effect of reflux time depended on the value of MPTMS amount and they were also responsible for changes in the monoglyceride selectivity.

A graphical representation of this 3D response curve is depicted in Fig. 12. The figure shows that for the shortest

Fig. 12 Response surface plot for monoglyceride selectivity (a) and its contour plot (b)



period of reflux time (4 h), monoglyceride selectivity increased initially with MPTMS amount, and then reached a maximum point at MPTMS amount of 3 mL per gram SBA-15. After that, it decreased significantly. A plausible explanation was based on results in Table 2 that suggest that the increase of MPTMS amount from 1 to 3 mL per gram SBA-15 resulted in a reduction of micropore area in the SBA-15SO₃H(5) catalyst. Meanwhile, excess MPTMS amount caused had dramatic increase in micropore area.

At long reflux time (20 h), different behaviours were observed. Initially, selectivity to monoglyceride decreased significantly with the MPTMS amount until the quantity of MPTMS was 3 mL per gram SBA-15. Then, it increased slightly at higher amount of MPTMS (5 mL per gram SBA-15). This could be explained based on FT-IR spectra analysis as shown in the Fig. 3. It suggests that the MPTMS amount of more than 1 mL per gram SBA-15 was related to weaker C–H stretching vibrations in the modified SBA-15 catalysts. This observation indicated lower amount of propyl sulfonic acid that had been successfully grafted on the modified SBA-15 catalysts.

In summary, the MPTMS amount was more significant parameter of the modified SBA-15 preparation conditions than the reflux time. Both parameters gave effects on micropore area, average pore diameter, acid site populations, etc. and consequently affected their catalytic activities. An increase in the catalytic activity of SBA-15SO₃H catalysts was mainly attributed to the lower of micropore structures and the higher amount of propyl sulfonic acid groups which were successfully grafted in the catalysts. The high amount of propyl sulfonic acid groups grafted in the catalysts led to the high amount of acid site populations in the catalysts. On the other hand, high amount of micropore structures in the modified SBA-15 catalysts resulted in the poor activity of the catalysts. It was due to severe restriction for formation and diffusion of bulky monoglyceride molecules through the microstructures where the acid sites were located. The effective acid sites could be lower than the total acid sites detected.

Finally, on the basis of graphical representation of the three-dimensional response surfaces and contour plots illustrated in Figs. 11 and 12, the highest monoglyceride selectivity (70.2%) coupled with excellent corresponding lauric acid conversion (around 95%) were achievable by the use of SBA-15SO₃H(1) catalyst prepared at reflux time of 20 h and the MPTMS amount of 1 mL per gram SBA-15.

Previously, SBA-15SO₃H prepared via direct synthesis was reported to give only 50% conversion and 57% selectivity to monoglyceride in the glycerol esterification with oleic acid at 120 °C for 24 h reaction [17]. Furthermore, in the esterification carried out at 150 °C for 6 h, the SBA-15SO₃H catalyst gave 93% fatty acid conversion but

lower selectivity to monoglyceride (around 20%). Thus, the SBA-15SO₃H(1) catalysts reported here showed better results for the catalytic activity.

4 Conclusions

Effects of different MPTMS amounts and reflux times used in the preparation conditions of propyl sulfonic acid functionalized SBA-15 catalysts (SBA-15SO₃H) were evaluated when used for esterification of lauric acid with glycerol. Successful acid functionalization of SBA-15 and the effects of synthesis conditions on their activity were demonstrated using a 3² factorial design. A mathematical model was successfully developed to simulate the catalysts activity in terms of lauric acid conversion and monoglyceride selectivity. Then, response surface plots were generated to show curvilinear plots of the lauric acid conversion and monoglyceride selectivity with both reflux time and MPTMS amount. The most critical factor in the catalyst preparations to eventually affect the catalytic activity was the MPTMS amount. The increase in the catalytic activity of SBA-15SO₃H catalysts was attributed to a decrease in micropore area and an increase in the amount of propyl sulfonic acid groups successfully grafted on the surface of the catalysts. As confirmed by the 3D response surfaces and their counter plots, SBA-15SO₃H(1) catalyst prepared at a reflux time of 20 h and an MPTMS amount of 1 mL per gram SBA-15 gave the highest monoglyceride selectivity (70.2%) with excellent lauric acid conversion (95%) in the glycerol esterification reaction.

Acknowledgments A Short Term (No.6035274) and a Research University (RU) grants (No.814003 and 814004) from Universiti Sains Malaysia to support this work are gratefully acknowledged.

References

1. N. Garti, A. Asein, M. Fanum, A DSC study of water behavior in water-in-oil microemulsions stabilized by sucrose esters, butanol. *Colloids Surf. A* **170**, 1–18 (2000)
2. L. Sagalowicz, M.E. Leser, H.J. Watzke, M. Michel, Monoglyceride self assembly structures as delivery vehicles. *Trend Food Sci. Technol.* **17**, 204–214 (2006)
3. H. Moonen, H. Bas, *Mono- and Diglycerides, Emulsifiers in Food Technology* (Oxford, Blackwell, 2004), pp. 40–58
4. C.A. Ferretti, R.N. Olcese, C.R. Apesteguia, J.I.D. Cosimo, Heterogeneously-catalyzed glycerolysis of fatty acid methyl esters: reaction parameter optimization. *Ind. Eng. Chem. Res.* **48**, 10387–10394 (2009)
5. N. Sanchez, M. Martinez, J. Aracil, Selective esterification of glycerine to 1-glycerol monooleate: 1. Kinetic modelling. *Ind. Eng. Chem. Res.* **36**, 1524–1528 (1997)
6. W.D. Bossaert, D.E.D. Vos, W.M.V. Rhijn, J. Bullen, Mesoporous sulfonic acids as selective heterogeneous catalysts for the synthesis of monoglycerides. *J. Catal.* **182**, 156–164 (1999)

7. C.S. Caetano, I.M. Fonseca, A.M. Ramos, J. Vital, J.E. Castanheiro, Esterification of free fatty acids with methanol using heteropolyacids immobilized on silica. *Catal. Commun.* **9**, 1996–1999 (2008)
8. R. Nakamura, K. Komura, Y. Sugi, The esterification of glycerine with lauric acid catalysts by multi-valent metal salts. Selective formation of mono- and dilaurins. *Catal. Commun.* **9**, 511–515 (2008)
9. L. Guerreiro, J.E. Castanheiro, I.M. Fonseca, R.M. Martin-Aranda, A.M. Ramos, J. Vital, Transesterification of soybean oil over sulfonic acid functionalised polymeric membranes. *Catal. Today* **118**, 166–171 (2006)
10. J. Aracil, M. Martinez, N. Sanchez, A. Corma, Formation of a jojoba oil analog by esterification of oleic acid using zeolites as catalyst. *Zeolites* **12**, 233–236 (1992)
11. E. Heykants, W.H. Verrelst, R.F. Parton, P.A. Jacobs, Shape-selective zeolite catalysed synthesis of monoglycerides by esterification of fatty acids with glycerol. *Stud. Surf. Sci. Catal.* **105**, 1277–1284 (1997)
12. Y. Pouilloux, S. Abro, C. van Hove, J. Barrault, Reaction of glycerol with fatty acids in the presence of ion-exchange resins: Preparation of monoglycerides. *J. Mol. Catal. A: Chem.* **149**, 243–254 (1999)
13. J. Perez-Pariente, I. Diaz, F. Mohino, E. Satre, Selective synthesis of monoglycerides by using functionalised mesoporous catalysts. *Appl. Catal. A* **254**, 173–188 (2003)
14. S.M. Stevens, K. Jansson, C. Xiao, S. Asahina, M. Klingstedt, D. Grüner, Y. Sakamoto, K. Miyasaka, P. Cubillas, R. Brent, L. Han, S. Che, R. Ryoo, D. Zhao, M. Anderson, F. Schüth, O. Terasaki, An appraisal of high resolution scanning electron microscopy applied to porous materials. *JEOUL News* **44**, 17–22 (2009)
15. W.M. van Rhijn, D.E. Vos, W.D. Bossaert, J. Bullen, B. Vouters, P. Grobert, P.A. Jacobs, Sulfonic acid bearing mesoporous materials as catalysts in furan and polyol derivatization. *Stud. Surf. Sci. Catal.* **117**, 183–190 (1998)
16. I. Hannus, M. Búza, A. Beck, L. Guzzi, G. Sáfrán, Hydrodechlorination catalytic activity of gold nanoparticles supported on TiO₂ modified SBA-15 investigated by IR spectroscopy. *J. Molec. Struct.* **924–926**, 355–357 (2009)
17. I. Diaz, F. Mohino, E. Satre, J. Perez-Pariente, Synthesis and catalytic properties of SO₃H-mesoporous materials from gels containing non-ionic surfactants. *Stud. Surf. Sci. Catal.* **135**, 1383–1390 (2001)
18. F. Hoffmann, M. Corneliu, J. Morell, M. Froba, Silica-based mesoporous organic–inorganic hybrid materials. *Angew. Chem. Int. Ed.* **45**, 3216–3251 (2006)
19. N. Garcia, E. Benito, J. Guzman, P. Tiemblo, V. Morales, R.A. Garcia, Functionalization of SBA-15 by an acid-catalyzed approach: A surface characterization study. *Micropor. Mesopor. Mater.* **106**, 129–139 (2007)
20. D. Zhao, Q. Huo, J. Feng, B.F. Chmelka, G.D. Stucky, Nonionic triblock and star diblock copolymer and oligomeric surfactant syntheses of highly ordered, hydrothermally stable mesoporous silica structures. *JAOCS* **120**, 6024–6036 (1998)
21. G.E.P. Box, W.G. Hunter, J.S. Hunter, *Statistics for experiments, an introduction to design, data analysis and model building* (Wiley, New York, 1978)
22. R. Molina, F. Martínez, J.A. Melero, D.H. Bremner, A.G. Chakinala, Mineralization of phenol by a heterogeneous ultrasound/Fe-SBA-15/H₂O₂ process: Multivariate study by factorial design of experiments. *Appl. Catal. B.* **66**, 198–207 (2006)
23. D. Das, J.F. Lee, S. Cheng, Selective synthesis of Bisphenol-A over mesoporous MCM silicacatalysts functionalized with sulfonic acid groups. *J. Catal.* **223**, 152–160 (2004)
24. T. Kang, Y. Park, J. Yi, Highly Selective adsorption of Pt²⁺ and Pd²⁺ using thiol-functionalized mesoporous silica. *Ind. Eng. Chem. Res.* **43**, 1478–1484 (2004)
25. C.M. Crudden, M. Sateesh, R. Lewis, Mercaptopropyl-modified mesoporous silica: A remarkable support for the preparation of a reusable, heterogeneous palladium catalyst for coupling reactions. *J. Am. Chem. Soc.* **127**, 10045–10050 (2005)
26. L. Hermida, A.Z. Abdullah, A.R. Mohamed, Post-synthetically functionalized SBA-15 with sulfonic acid and sulphated zirconia for esterification of glycerol to monoglyceride. *J. Appl. Sci.* **10(24)**, 3199–3206 (2010)
27. Y.C. Yang, S.R. Vali, Y.H. Ju, A process for synthesizing high purity monoglyceride. *J. Chin. Inst. Chem. Eng.* **34**, 617–623 (2003)
28. W. Volland, Organic compound identification using infrared spectroscopy, available from World Wide Web: <http://www.800mainstreet.com/irsp/eir.html> (accessed on August 2010)
29. M. Kruk, M. Jaroniec, C.H. Ko, R. Ryoo, Characterization of the porous structure of SBA-15. *Chem. Mater.* **12**, 1961–1968 (2000)
30. B. Rac, P.F. Molnar, M. Mohai, I. Bertoti, A comparative study of solid sulfonic acid catalysts based on various ordered mesoporous silica materials. *J. Molec. Catal. A* **244**, 46–57 (2006)
31. M.C. Chao, C.H. Chang, H.P. Lin, C.Y. Tang, C.Y. Lin, Morphological control on SBA-15 mesoporous silicas via a slow self-assembling rate. *J. Mater. Sci.* **44**, 6453–6462 (2009)
32. W. Cao, C. Zhang, P. Hong, H. Ji, Response surface methodology for autolysis parameters optimization of shrimp head and amino acids released during autolysis. *J. Food Chem.* **109**, 176–183 (2008)